Large variations in the propensity of aqueous oxychlorine anions for the solution/vapor interface

Niklas Ottosson[a,*], Robert Vácha[b], Emad F. Aziz[c], Wandared Pokapanich[a], Wolfgang Eberhardt[c], Svante Svensson[a], Gunnar Öhrwall[d], Pavel Jungwirth[b,*], Olle Björneholm[a], and Bernd Winter[c,*]

[a]*Department of Physics and Materials Science, Uppsala University, SE-751 21 Uppsala, Sweden*
[b]*Institute of Organic Chemistry and Biochemistry, Academy of Sciences of the Czech Republic, and Center for Biomolecules and Complex Molecular Systems, Flemingovo nám. 2, 16610 Prague 6, Czech Republic*
[c]*Helmholtz-Zentrum Berlin für Materialien und Energie, and BESSY, Albert-Einstein-Strasse 15, D-12489 Berlin, Germany*
[d]*MAX-lab, Lund University, Box 118, SE-221 00 Lund, Sweden*

Keywords: Aqueous solution, Water, Interfacial structure, Surface segregation, Oxychlorine anion, X-ray Photoelectron Spectroscopy, Molecular Dynamics

Abstract

Core-level photoelectron spectroscopy measurements have been performed of aqueous solutions of NaCl co-dissolved with $NaClO_n$ (n = 1-4). Each species has a distinct Cl 2*p* electron binding energy, which can be exploited for depth-profiling experiments to study the competition between Cl^- and ClO_n^- anions for residing in the outermost layers of the solution/vapor interface. Strongest propensity for the surface is observed for n = 4 (perchlorate), followed by n = 3 (chlorate), n = 2 (chlorite), n = 0 (chloride), and n = 1 (hypochlorite). Molecular dynamics simulations rationalize the greatest surface propensity of the most oxidized anions in terms of their larger size and polarizability. The anomalous behavior of hypochlorite, being less surface-active than chloride, though it is both larger and more polarizable, is suggested to arise from the charge asymmetry over the anion, increasing its efficiency for bulk solvation.

*Corresponding authors: niklas.ottosson@fysik.uu.se (N.O.), pavel.jungwirth@uochb.cas.cz (P.J.) and bernd.winter@bessy.de (B.W.)

1 Introduction

Understanding the details of which parameters govern ion specific surface phenomena is of both fundamental and practical importance, e.g. for developing better models of atmospheric chemical reactions at the surface of aqueous mesoscopic aerosols. The surface propensity of chloride for the aqueous surface has attracted special attention due to its omnipresence in seawater, being a precursor for photochemical reactions leading to the formation of gaseous chlorine.[1] Recently, both experimental and theoretical studies have been performed in order to elucidate the photochemical oxidation reactions of chloride leading to the formation of atmospheric perchlorate through intermediate steps, involving reactive oxychlorine anions of lower oxygen coordination numbers.[2,3] The details of these transformation processes are not well understood, and even though the formation of chlorine radicals on the surface of salt aerosols is well documented, the exact nature of the chemical pathways remains unresolved.[3] In order to better understand these processes, and in particular to evaluate the importance of different oxychlorine anions as precursors (and their potential role in reactions with gaseous particles, such as ozone), it is crucial to determine the spatial distribution of the various species in the interfacial region.

During recent years, a number of observations were made that contradict classical electrostatic models, developed to explain the molecular structure of aqueous salt solution interfaces.[4] Two important predictions of these models are that the solution interface is i) essentially free of ions, and ii) that the solute density variation in the surface region is not strongly ion specific (and mainly varies with salt concentration). Recent data have shown, however, that aqueous ions seem to not only penetrate into the outermost surface layers – appreciable ion specificity in the interfacial density variations has also been observed. Moreover, certain inorganic ions may even be *enriched* at the topmost layer as compared to the bulk solution.[5-7]

Photoelectron spectroscopy (PES) can be used to study local solute density variations over a sizeable range of probing depths, simply by exploiting the electron mean free path's dependence on kinetic energy (KE) in the condensed phase.[8,9] In the present work we study aqueous solutions of NaCl, co-dissolved with various sodium oxychlorine salts. By the chemical sensitivity achieved in PES, chlorine atoms of the different anions can be distinguished. Thus, local density variations near the solution interface can be probed through the relative Cl photoemission signals.

When comparing depth profiles of two solutes composed of different elements, ionization cross sections and angular anisotropy parameters, which vary as function of the excitation energy and the electron detection geometry, must be taken into account – quantities which are poorly understood for ions in the aqueous phase.[10] In this work the situation simplifies considerably since we exclusively measure the Cl *2p* core-level photoemission signal intensity. Then, signal ratios of the various oxychlorine anions relative to the chloride anion as function of excitation energy can be determined without running into the aforementioned complications. Such measurements provide no direct information about the absolute distribution of the oxychlorine anions in the interfacial region since the density function of the chloride reference is not measured independently. However, we can monitor differences in the propensity of the oxychlorine anions for the aqueous surface depending on the oxygen coordination number. We have chosen the Cl^- anion as reference since it has been extensively studied,[11,12] being the simplest and most common chlorine-containing anion.

From PES measurements of 1m NaCl, co-dissolved with 1m $NaClO_n$ (n = 1-4) in water, we show that the surface propensity of an aqueous oxychlorine anion ClO_n^- strongly depends on the oxygen coordination number n. A concentration of 1m Cl, as used here, is not atypical to what is found in seawater-born atmospheric species. Although the oxychlorine anion concentration in these aerosols is typically considerably lower than 1m, the surface segregation behavior discussed in the present work, qualitatively applies to lower

concentrations as well. Perchlorate (n = 4) is found to be enriched strongest at the surface, closely followed by chlorate (n = 3), chlorite (n = 2), chloride (n = 0) and hypochlorite (n = 1). With the exception of hypochlorite, the relative surface coverage thus decreases with the anion size. Molecular dynamics (MD) simulations of an aqueous solution consisting of 1m NaCl co-dissolved with 1m $NaClO_4$ qualitatively corroborate the experimental observations, which can be explained in terms of differences in size and polarizability of the two anions. Even though hypochlorite is found to have just a slightly lower propensity for the surface compared to chloride, the anomalous behavior of ClO^-_{aq} may point to another competing mechanism important for ion specific surface phenomena. We suggest that the appreciable charge asymmetry on the hypochlorite anion is playing an important role, increasing its bulk solubility, and consequently reducing its propensity for the aqueous surface. The present study demonstrates how a subtle competition between different mechanisms governs the molecular surface structure of aqueous solutions.

2 Methods

2.1 Experimental

The X-ray PES studies from mixed 1m NaCl / 1m $NaClO_n$ aqueous solution were conducted using soft X-ray photons from the U41-PGM undulator beamline of the synchrotron facility BESSY, Berlin. The target was a 15 μm liquid micro-jet at 4^{o}C, injected into vacuum and traveling at a velocity of approximately 100 m/s. Under these conditions the loss of photoelectrons, originating from the aqueous phase, due to collision with gas-phase water molecules is minimized, and electron kinetic energies can be readily measured. Experimental details of the setup have been described previously.[13,14] Briefly, the synchrotron light polarization vector is parallel to the flow of the liquid jet, while perpendicular to the symmetry axis of the electron analyzer. The photoelectrons emitted from the liquid surface enter the differentially pumped electron analyzer through a skimmer with a diameter of 500

μm. Typical operation pressure is in the low 10^{-5} mbar range for the main experimental chamber, and in the low 10^{-7} mbar range for the spectrometer. The total experimental resolution was better than 250 meV, which was determined from the width of the $1b_1$ water gas-phase line. Solutions were prepared from highly demineralized water, and commercially available salts (NaCl, 99%. NaClO, purum; 10% in solution. $NaClO_2$, technical grade; 80%. $NaClO_3$, 99% and $NaClO_4$, 98%.) were obtained from Sigma-Aldrich and used without any further purification.

All Cl 2*p* spectra were fitted using post-collision interaction (PCI) line shapes, using the analytical form as developed in.[15] Asymmetry parameters and Lorentzian line widths were kept fixed in the fits, and the Cl 2*p* lifetime was taken from experimental gas-phase values from the literature.[16] Energy positions and intensities of each spin-orbit doublet component were free parameters in the fitting procedure. The Gaussian width was free for each doublet, but the constituent components were forced to the same value. All electron binding energies (BE) reported here are with respect to vacuum, and were calibrated against the $1b_1$ state of liquid water.[13]

2.2 Molecular dynamics simulations

In order to shed light on the microscopic origins of the mechanisms governing ion specific preferential surface segregation we have performed a MD simulation of a mixed 1m NaCl / 1m $NaClO_4$ solution, i.e., the smallest and largest chlorine anion considered in the present experimental work. The system consisted of 1443 water molecules, 52 Na^+, 26 Cl^-, and 26 ClO_4^- ions. This system was placed in a prismatic unit cell of dimensions 2.83 x 2.83 x 21.4 nm. Periodic boundary conditions were applied, yielding an infinite slab with two water/vapor interfaces. After nanosecond-timescale equilibration, data were collected over a 40 ns long simulation time. Simulations were performed with a 1 fs time step in the NVT ensemble at 300 K, using the Berendsen temperature coupling.[17] All interactions were cut off

at 1.1 nm, and long-range electrostatic effects were included through the smooth particle Mesh Ewald method.[18] For water we have employed the polarizable POL3 model.[19] The force field parameters employed for the polarizable ions are presented in Table 1. For perchlorate, parameterization was based on MP2/aug-cc-pvtz calculations employing a polarizable continuum model for the aqueous solvent. In the MD simulations, the ion was kept rigid at tetrahedral geometry with the Cl–O bond length fixed at 1.50 Å. The simulations were performed using the Gromacs program package (version 3.3.1), compiled in double precision.[20]

3 Results

3.1 Cl 2*p* photoelectron spectra

Figure 1 contrasts the Cl 2*p* PE spectra from aqueous solutions of NaCl/$NaClO_n$ (n = 1-4) obtained at photon energies 308 eV (blue curves) and 1108 eV (red curves). All BE and full widths at half maximum (fwhm) values obtained from fitting the spectra are summarized in Table 2. In comparing the traces one finds considerable changes of the Cl 2*p* intensities from the different $ClO_n^-{}_{aq}$ anions relative to Cl^-_{aq} as a function of n. For hν = 308 eV, the ClO_4/Cl PE signal ratio is as large as 1.95, dropping to 1.92, and 1.41 for ClO_3/Cl and ClO_2/Cl, respectively. Since the bulk concentrations of Cl^-_{aq} and $ClO_n^-{}_{aq}$ are the same, 1m, ratios larger than 1 indicate a higher interfacial concentration of $ClO_n^-{}_{aq}$, n = 2-4, as compared to Cl^-_{aq}. Thus relative interfacial concentrations seem to increase with oxygen coordination number.

The situation is somewhat more complicated for the ClO^-/Cl^- solution (trace d). First, emission from the two anions overlaps (the fits included at the bottom of the figure show the decomposition of the superimposed spectral features). We therefore have to assume that the chloride line shape is the same as for the other solutions, which indeed results in good fits for all spectra. Further, hypochlorite gradually disproportionates in water, $3\ ClO^-_{aq} \rightarrow ClO_3^-{}_{aq} + 2$

Cl^-_{aq} and 2 $ClO^-_{aq} \rightarrow O_{2,aq}$ + 2 Cl^-_{aq},[21] leading to the additional small $ClO_3^-{}_{aq}$ peaks at 211.3 and 212.9 eV as well as to an appreciable increase of the Cl^- 2*p* intensity. As a consequence, the macroscopic proportion of ClO^- to Cl^- is not 1:1, but rather close to 1:2. As the disproportion might conceivably have progressed during the time of the measurements (which would appear as an artificial variation of the solute composition with probing depth) we recorded additional control spectra of Cl 2*p* and of the valence band of the solutions in the beginning and the end of the experimental series. No temporal changes were observed, and hence the solute composition was constant throughout data collection.

The electron signal measured in a PE experiment is proportional to $\int \rho(z)\cdot\exp(-z/\mathrm{IMFP})\, dz$, where ρ is the density of the measured species as function of distance z from the interface. IMFP denotes the electron inelastic mean free path that strongly depends on eKE, and this property is exploited in depth profiling photoemission experiments. The IMFP can be varied over a significant range of distances by suitable choice of the excitation photon energy – from a few Ångströms to tens of nanometers.[22] Figure 1 shows two superimposed spectra for each solution, measured at 308 and 1108 eV photon energy, respectively, and demonstrates the effects of IMFP variation for the different ClO_n^-/Cl^- mixed solutions. Intensities have been normalized to the chloride doublet-peak in all spectra. With BEs of approximately 208 eV on average, the resulting photoelectrons have roughly 100 eV (short IMFP, surface sensitive) and 900 eV (larger IMFP, more bulk sensitive) kinetic energies, respectively. The peaks originating from the oxychlorine anions show pronounced intensity variations relative to chloride at the two different photon energies. The decrease of the $ClO_n^-{}_{aq}$ signal with larger IMFP in traces (a)-(c) shows that $ClO_4^-{}_{aq}$, $ClO_3^-{}_{aq}$ and $ClO_2^-{}_{aq}$ are relatively surface enhanced, and that this enhancement scales with *n*. The intensity variation in trace (d), however, seems to indicate the contrary behavior of what was found for the other three solutions. The ClO^-_{aq} PE signal intensity is *higher* in the spectra taken at higher photon energy (more bulk

sensitive), suggesting that the hypochlorite anion actually has a *lower* surface propensity compared to chloride.

In order to follow the dependence of the relative anion PE signal ratios with variation of electron mean free path more systematically, we have recorded Cl 2*p* spectra from the four solutions at a number of different photon energies, covering the 50-900 eV KE range. For each spectrum the respective components were fitted as described above, and the fits were thereafter integrated. The resulting ClO_n^-/Cl^- PE signal ratios as function of KE are given in Figure 2. For n = 2-4 the ratios reach a maximum value at 100 eV KE, which apparently corresponds to a minimum in the IMFP values. For KEs both higher and lower than 100 eV the PE signal ratios drop, clearly showing that the larger oxychlorine anions are surface enhanced relative to the chloride.[23]

As already pointed out, the hypochlorite behaves very different compared to the other oxychlorine anions. The ClO^-/Cl^- ratios in Figure 2 drop from 0.7 to 0.43 when going from 50 to 200 eV KE, and then the ratios slowly increase up to a value of 0.5 at 900 eV KE. The overall trend of the curve, exhibiting a washed out minimum, is thus inversed compared to the curve of the larger oxychlorine anions, exhibiting a maximum. This directly shows that ClO^-_{aq} has a lower propensity for the liquid/vapor interface than chloride, which we had already speculated based on the spectra of Figure 1. As explained earlier, it is the *differences* in the ClO_n^-/Cl^- PE intensity ratio as function of the electron KE that reflects variations in the surface coverage of the two ions – not the absolute values. The fact that the ClO_n^-/Cl^- ratios converge toward 0.5 at high KEs (instead of unity as for the other ions) merely reflects the approximate macroscopic 1:2 hypochlorite/chloride proportions.[24]

3.2 Molecular dynamics simulations

Figure 3 depicts a typical snapshot of one of the two equivalent halves of the simulated slab, showing an instantaneous distribution of chloride, perchlorate and sodium ions, as well

as water molecules. Partial density profiles of the individual species, symmetrized over the two equivalent halves of the slab and averaged over the whole trajectory, are presented in Figure 4a. For visual clarity the water density is set to unity in the center of the slab and all ion density profiles are normalized such that they have the same integral value. As seen in Figure 4a, perchlorate on average reaches further out to the interface compared to chloride. Importantly, ClO_4^- displays a rather distinct surface density peak, reflecting affinity of this anion for the solution water surface. Due to electrostatic attraction, sodium exhibits a sub-surface peak (not shown in the figure), resulting form charge neutralizing forces from the anions. At the relatively high concentrations in the current simulation, we have observed occasional clustering of perchlorates with sodium counterions in the bulk. This weak clustering, which could result from inaccuracies in the force field, may artificially reduce the surface propensity of ClO_4^-.

As such, the density profiles in Figure 4a cannot directly be compared with the PE data in Figures 1 and 2. However, when convoluted with an exponential decaying IMFP attenuation function the density function can be used to extract simulated photoelectron intensity distributions. In Figure 4b we show two illustrative examples of PE distributions, assuming IMFP values of 5 and 10 Å, respectively. As previously mentioned the experimental PE signal can be described as the integral of such photoelectron distribution, and allows for a more direct comparison with the PES data.[10] When integrated, the distributions in Figure 4b yield simulated ClO_4^-/Cl^- PE ratios of 1.12 and 1.02 for 5 and 10 Å IMFP, respectively, which is significantly lower than 1.95 observed experimentally at 100 eV KE. This will be discussed further below.

Finally, we like to comment on a specific observation on the water-perchlorate interaction geometry in the simulations. Let's consider the spatial distribution of water hydrogens and oxygens around all ClO_4^- ions, averaged over the whole simulation time, as shown in Figure 5. We see that the tetrahedral symmetry of the perchlorate anion induces

preferential orientations of solvent molecules in the first solvation shell, with water hydrogens filling positions in the vertices of the tetrahedron next to oxygens of perchorate while water oxygens are filling positions in-between the vertices. This reveals a relatively structured hydration shell of ClO_4^-, as opposed to the spherical solvent shell of chloride. The photoelectron spectra shown in Figure 1 also show a monotonous decrease of the Cl 2*p* peak widths as a function of *n* – see Table 1 for values. This is primarily due to the more rigid configurations imposed by the covalently bonded oxygens in ClO_n^- for higher *n*, but could also be indicative of more well defined interaction geometry with water molecules in the first solvation shell at higher oxygen coordination numbers, i.e., in excellent agreement with the situation depicted in Figure 5. Hydration of the bare chloride anion, i.e., $Cl^-(H_2O)_x$ in contrast allows for a larger variation of solvation-shell configurations (both in coordination number and hydrogen bonding geometries), each with a slightly varying Cl 2*p* BE, leading to a broader photoemission feature.

4 Discussion

Moberg and co-workers have investigated the surface structure of phase-transfer catalysts in formamide solution by angle-resolved photoemission.[25] In a 1:1 solution of perchlorate and chloride, with the surface-active tetrabutylammonium (TBA) molecule as the counter-ion, they observed an appreciable surface enhancement of perchlorate, more pronounced than what was found here. This enhancement was attributed to perchlorate ion pairing with the TBA cation and the formation of strong surface complexes. While this conclusion still holds, the present PE data shows how strong the preferential surface segregation of large polarizable anions can be, even in the absence of the electrostatic attraction of surface-active counter ions. In the MD simulation of NaCl co-dissolved with $NaClO_4$, this behavior could be qualitatively reproduced. The difference in surface coverage of Cl^- compared to ClO_4^- is a consequence of the differences in size and polarizability of the

ions. In our previous simulation study of aqueous NaI[26] we have artificially decoupled the two effects. We have shown for iodide that both size (leading to unfavorable solvent exclusion) and polarizability (of the ion and of water) contribute to the surface affinity of iodide. We anticipate that this is true also for other soft anions, such as perchlorate.

Assuming a very short value of 5 Å for the IMFP, the density profiles shown in Figure 4a yield a simulated ClO_4^-/Cl^- PE signal ratio of 1.12. In order to reproduce the experimental value of 1.95, obtained at 100 eV KE, a IMFP value of 1.4 Å has to be assumed. This is unrealistically short, even for compact metals,[22] and about one order of magnitude lower than what has been suggested to be the minimum value from recent experimental estimates of pure liquid water.[10] Quantitatively, the experiments thus reveal a significantly larger relative perchlorate surface propensity than expected from our calculations. This discrepancy is likely due to inaccuracies in the empirical force field. Indeed, the exact affinity of an ion for the air/water interface depends on a particular choice of interaction potential. However, the real dividing line goes between polarizable and non-polarizable force fields. Semiquantitatively, the former show an appreciable propensity for the surface of large soft inorganic ions (e.g., iodide, bromide, and to a lesser extent also chloride), while the surface effect is significantly reduced for the latter.[27] It seems that the present perchlorate potential, albeit polarizable, still to a certain extent underestimates the surface affinity of this ion, which may also be due to a too strong sodium-perchlorate pairing and even occasional clustering during the simulation.

How can we understand the anomalous behavior of hypochlorite, being both larger and more polarizable than chloride but still having a lower propensity for the interfacial region? We believe that this is a consequence of the oxychlorine anion's dipole moment. Since multipole expansions are ill-defined for charged species – the net charge makes the coefficients dependent on the choice of spatial origin – we discuss this effect in terms of partial (Mulliken) charges. These amount to -0.12 and -0.88 *e* for the Cl and O atoms, respectively, and it is this emerging charge asymmetry that may lead to increased bulk

solubility, and hence to a reduced surface propensity of ClO^-. Investigating this hypothesis by classical MD simulations is problematic, though, due to the chemical reactivity of the hypochlorite anion. For this reason, no force field is available for hypochlorite, and the usual way of potential parameterization against *ab initio* calculations for small clusters is hardly feasible.

In explaining the unexpected behavior of ClO^- we have not yet considered the possibility that chlorine-containing species other than the ones discussed above may form in solution, but staying undetected due to spectral overlap. Such species might have different surface propensity than the oxychlorine anions considered, possibly leading us to draw inaccurate conclusions about the behavior of ClO^-. However, the only reasonable potential candidate we can propose is HOCl, the conjugate acid to the hypochlorite anion ($HOCl_{aq} \leftrightarrow ClO^-_{aq} + H^+_{aq}$), which indeed may have very different surface properties than ClO. Yet, this species can be ruled out here because the ClO^-/Cl^- solution is very basic (pH 11).

5 Conclusions

The present photoemission data supported by MD simulations have unambiguously shown that the larger oxychlorine anions exhibit considerably higher propensities for the aqueous interface than chloride, rationalized in terms of their larger size and polarizability. The anomalous behavior of hypochlorite, found to be the least surface active of the investigated chlorine containing anions even though it is both larger and more polarizable than chloride, has been tentatively explained by the charge asymmetry on the ClO^- anion, thus illustrating the competition of several different mechanisms governing ion specific surface segregation. These considerations must surely be taken into account when fully modeling the photochemical pathways leading to the formation of perchlorate in aqueous aerosols and at other aqueous systems where surfaces are important. The present work also illustrates the

potential of photoelectron spectroscopy to become an important technique for measuring local density variations of solutes in aqueous solutions.

Note added in proof

After submission of this manuscript our attention was drawn to a similar work, recently submitted to Journal of Physical Chemistry C, albeit solely addressing aqueous chloride and perchlorate.[28] Results are in agreement with our conclusions.

Acknowledgments

Financial support is gratefully acknowledged from the European Research Area, through EU-I3 funding program Project 2007-2-70521, the Swedish Research Council (VR), The Knut and Alice Wallenberg Foundation, Göran Gustafssons Foundation, the Carl Tryggers Foundation, the Swedish Foundation for Strategic Research (SSF), NordForsk and the Thai Royal government. This work was further supported by the Czech Science Foundation (Grant No. 203/08/0114) and the Czech Ministry of Education (Grant No. LC512). R.V. acknowledges support from the International Max-Planck Research School. Part of the work in Prague was supported via Project No. Z40550506. B.W. gratefully acknowledges support from the Deutsche Forschungsgemeinschaft (project WI 1327/3-1). We also would like to thank the BESSY staff for helpful assistance during the experiments.

Figure and table captions

Figure 1) Cl 2*p* photoemission spectra from aqueous solutions of $NaClO_n$, n = 1-4, co-dissolved with NaCl, with total salt concentrations of 2 (1+1) molal. (a) $NaClO_4$/NaCl, (b) $NaClO_3$/NaCl, (c) and $NaClO_2$/NaCl. Due to disproportion (see text) the mole ratio of ClO^- to Cl^- (trace d) was instead near 1:2, and remains constant during the measurements. Blue curves are the spectra measured at 308 eV photon energies, corresponding to probing the solution interface. Red curves were measured at 1108 eV, and correspond to signal originating primarily from the bulk solution. Intensities in each trace were normalized at the Cl^-_{aq} 2*p* PE peak height.

Figure 2) Plot of experimental ClO_n^-/Cl^- PE ratios, as extracted from fits of Cl 2*p* spectra like those shown in Figure 1. Since the electron inelastic mean free path varies with kinetic energy of the photoelectrons, the variation in the signal ratios reflects differences in the relative surface propensity for the oxychlorine anions.

Figure 3) Snapshot from MD calculations of 1m $NaClO_4$ / 1m NaCl in water, showing the distribution of chloride, perchlorate, and sodium ions in half of the simulated aqueous slab. Na atoms are light green, Cl darker turquoise while the perchlorate oxygens are red.

Figure 4) a) Simulated density profiles (solid lines), extending from the center of the slab to the interface, of Cl^- and ClO_4^- anions in 1m $NaClO_4$ / 1m NaCl mixed aqueous solutions. b) shows corresponding calculated photoelectron signals for IMFP = 5 and 10 Å.

Figure 5) Distributions of water hydrogens (white) and oxygens (blue) around ClO_4^-, averaged over the whole MD trajectory.

Table 1. Force field parameters employed for ions in the present MD simulation.

Table 2. Cl *2p* binding energies and full widths at half maximum (fwhm) for the oxychlorine and chloride anions investigated in this work.

References

(1) Knipping, E. M.; Lakin, M. J.; Foster, K. L.; Jungwirth, P.; Tobias, D. J.; Gerber, R. B.; Dabdub, D.; Finlayson-Pitts, B. J. *Science* **2000**, *288*, 301.

(2) Dasgupta, P. K.; Martinelango, P. K.; Jackson, W. A.; Anderson, T. A.; Tian, K.; Tock, R. W.; Rajagopalan, S. *Environmental Science & Technology* **2005**, *39*, 1569.

(3) Kang, N.; Anderson, T. A.; Jackson, W. A. *Analytica Chimica Acta* **2006**, *567*, 48.

(4) Onsager, L.; Samaras, N. N. T. *Journal of Physical Chemistry* **1934**, *2*, 528.

(5) Jungwirth, P.; Tobias, D. J. *Journal of Physical Chemistry B* **2001**, *105*, 10468.

(6) Pegram, L. M.; Record, M. T. *Proceedings of the National Academy of Sciences of the United States of America* **2006**, *103*, 14278.

(7) Dang, L. X.; Chang, T. M. *Journal of Physical Chemistry B* **2002**, *106*, 235.

(8) Hüfner, S. *Photoelectron Spectroscopy: Principles and Applications*; Springer-Verlag: Berlin, Heidelberg, New York, London, Paris, Tokyo, Hong Kong, Barcelona, Budapest, 1995.

(9) Ghosal, S.; Hemminger, J. C.; Bluhm, H.; Mun, B. S.; Hebenstreit, E. L. D.; Ketteler, G.; Ogletree, D. F.; Requejo, F. G.; Salmeron, M. *Science* **2005**, *307*, 563.

(10) Ottosson, N.; Faubel, M.; Bradforth, S. E.; Jungwirth, P.; Winter, B. *J. Elect. Spectrosc. Relat. Phenom. In press.* **2009**.

(11) Winter, B.; Weber, R.; Hertel, I. V.; Faubel, M.; Jungwirth, P.; Brown, E. C.; Bradforth, S. E. *Journal of the American Chemical Society* **2005**, *127*, 7203.

(12) Winter, B.; Aziz, E. F.; Ottosson, N.; Faubel, M.; Kosugi, N.; Hertel, I. V. *J. Am. Chem. Soc.* **2008**, *130*, 7130.

(13) Winter, B.; Weber, R.; Widdra, W.; Dittmar, M.; Faubel, M.; Hertel, I. V. *Journal of Physical Chemistry A* **2004**, *108*, 2625.

(14) Winter, B. *Nuclear Instruments & Methods in Physics Research Section a-Accelerators Spectrometers Detectors and Associated Equipment* **2009**, *601*, 139.

(15) van der Straten, P.; Morgenstern, R.; Niehaus, A. *Zeitschrift Fur Physik D-Atoms Molecules and Clusters* **1988**, *8*, 35.

(16) Fink, R. F.; Kivilompolo, M.; Aksela, H.; Aksela, S. *Physical Review A* **1998**, *58*, 1988.

(17) Berendsen, H. J. C.; Postma, J. P. M.; Vangunsteren, W. F.; Dinola, A.; Haak, J. R. *Journal of Chemical Physics* **1984**, *81*, 3684.

(18) Essmann, U.; Perera, L.; Berkowitz, M. L.; Darden, T.; Lee, H.; Pedersen, L. G. *Journal of Chemical Physics* **1995**, *103*, 8577.

(19) Caldwell, J. W.; Kollman, P. A. *Journal of Physical Chemistry* **1995**, *99*, 6208.

(20) Lindahl, E.; Hess, B.; van der Spoel, D. *Journal of Molecular Modeling* **2001**, *7*, 306.

(21) Adam, L. C.; Fabian, I.; Suzuki, K.; Gordon, G. *Inorganic Chemistry* **1992**, *31*, 3534.

(22) Pianetta, P. *http://xdb.lbl.gov/section3/sec_3-2.html.*

(23) At a high enough KE, we would expect to obtain 1:1 signal ratios of ClO_n^- and Cl^- (n= 2-4), corresponding to the macroscopic stoichiometric proportions, given our assumption that the Cl 2*p* photoionization cross section is the same for all ionic species. While this assumption might not be fully accurate, e.g. due to small variations in the intensity of satellites which redistribute signal from the main PE line [8] different cross sections for the ions are highly unlikely to explain the ClO_n^-/Cl^- ratio of 1.2 at 900 eV KE. Rather, one must keep in mind that the photoemission signals are integrals of the total density distributions from the surface into the bulk, *exponentially* attenuated by the electron mean free path. In a recent photoemission study of aqueous NaI we have shown that the surface enhancement of iodide relative to sodium was observable only for electron KEs smaller than 600 eV; higher KEs primarily probe the bulk solution.[10] Probably, for the systems investigated here the preferential surface

segregation is significantly stronger than for NaI solutions, and hence surface contributions to the total signal remain detectable at the highest KE achieved here. It would require considerably higher KEs for the surface contributions to become negligible.

(24) While the rest of the ClO^-/Cl^- data set is consistent with a lower surface segregation of hypochlorite relative to chloride, the sharp jump in Figure 2 from 0.47 to 0.70 when going from 100 to 50 eV hardly seems consistent with the bulk stoichiometry of ClO^- to Cl^- – if the bulk ratio is 1:2 the PE ratio should not exceed 0.5. Neither can any single IMFP function explain this large variation with KE for hypochlorite, and at the same time account for the much smaller changes ClO_n^-/Cl^- in the same KE range for the larger oxychlorine anions. One possibility would be to assume a dramatic dependence of the IMFP values on the ionic species, but this assumption could hardly be physically justified. Rather, at 50 eV KE we are apparently too close to the ionization threshold for making the approximation that the effective Cl 2*p* cross section is ion-independent. In the condensed phase, low KE electrons can give rise to complex scattering phenomena and even in the gas phase severe dependence of the effective core-electron cross sections has been observed on the local molecular structure at the ionized site (Leif Saethre, private communication). Above 100 eV KE these effects should however be very small.

(25) Moberg, R.; Bokman, F.; Bohman, O.; Siegbahn, H. O. G. *Journal of the American Chemical Society* **1991**, *113*, 3663.

(26) Vrbka, L.; Mucha, M.; Minofar, B.; Jungwirth, P.; Brown, E. C. *Curr. Opn. Coll. Int. Sci.* **2004**, *9*, 67.

(27) Jungwirth, P.; Tobias, D. J. *Chemical Reviews* **2006**, *106*, 1259.

(28) Baer, M. D.; Kuo, I.-F. W.; Bluhm, H.; Ghosal, S. *J. Phys. Chem. C*, *(submitted 2009)*.

Atom	Charge [e]	Polarizability [nm^3]	σ [nm]	ε [kJ/mol]
Cl	-1.0000	0.001910	0.43200	0.4184
Na	1.0000	0.000240	0.235019	0.543920
ClO_4-Cl	1.120	0.000000	0.3563594872	1.046000
ClO_4-O	-0.530	0.001156	0.3203671790	0.652704

Table 1

Anion	Level	BE [eV]	fwhm [eV]
$ClO_4^-{}_{aq}$	Cl $2p_{3/2}$	213.4	0.95
	Cl $2p_{1/2}$	215.0	0.95
$ClO_3^-{}_{aq}$	Cl $2p_{3/2}$	211.3	0.99
	Cl $2p_{1/2}$	212.9	0.99
$ClO_2^-{}_{aq}$	Cl $2p_{3/2}$	208.7	1.01
	Cl $2p_{1/2}$	210.2	1.01
$ClO^-{}_{aq}$	Cl $2p_{3/2}$	205.7	1.10
	Cl $2p_{1/2}$	207.3	1.10
Cl^-	Cl $2p_{3/2}$	203.3	1.11
	Cl $2p_{1/2}$	204.8	1.11

Table 2

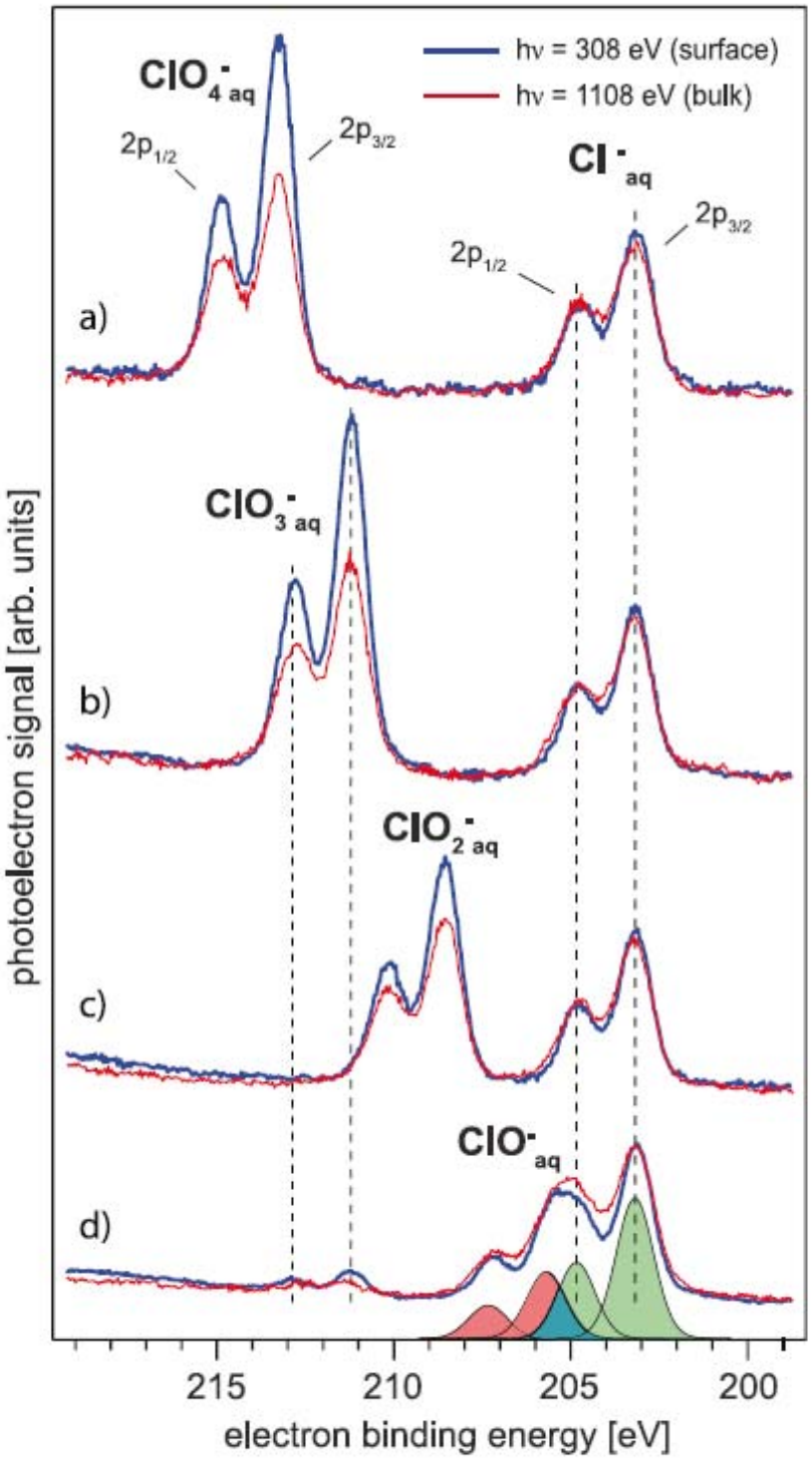
hν = 308 eV (surface)
hν = 1108 eV (bulk)
ClO4- aq
2p1/2
2p3/2
Cl- aq
2p1/2
2p3/2
a)
ClO3- aq
b)
ClO2- aq
c)
ClO- aq
d)
photoelectron signal [arb. units]
215
210
205
200
electron binding energy [eV]

Figure 1

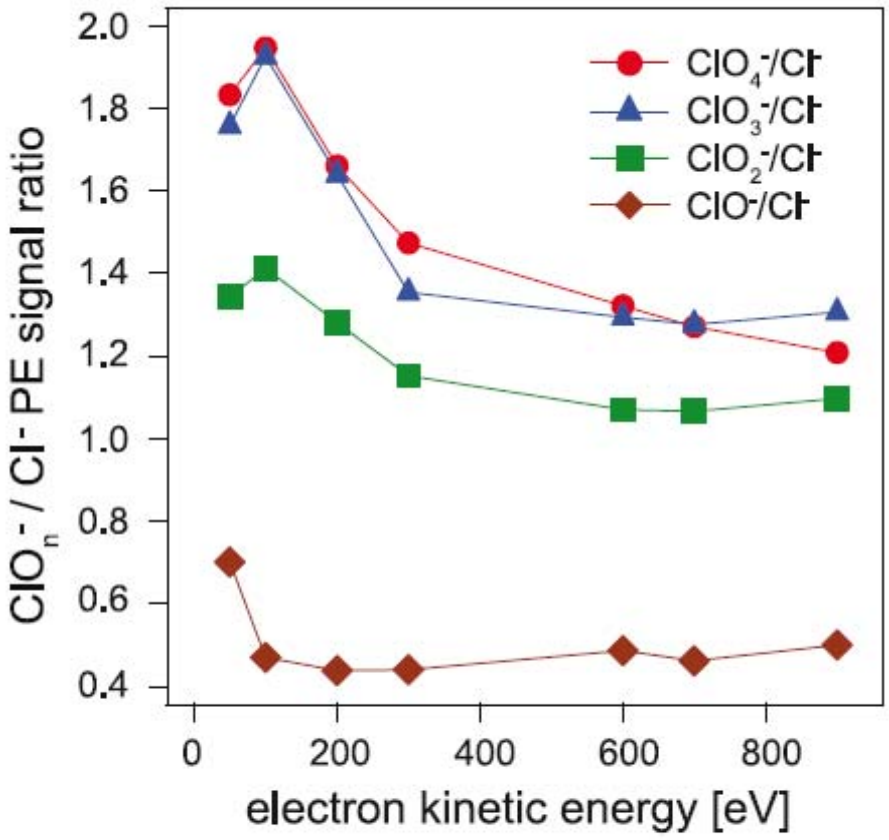
2.0
1.8
1.6
1.4
1.2
1.0
0.8
0.6
0.4
ClO$_n^-$ / Cl$^-$ PE signal ratio
0
200
400
600
800
electron kinetic energy [eV]
ClO$_4^-$/Cl$^-$
ClO$_3^-$/Cl$^-$
ClO$_2^-$/Cl$^-$
ClO$^-$/Cl$^-$

Figure 2

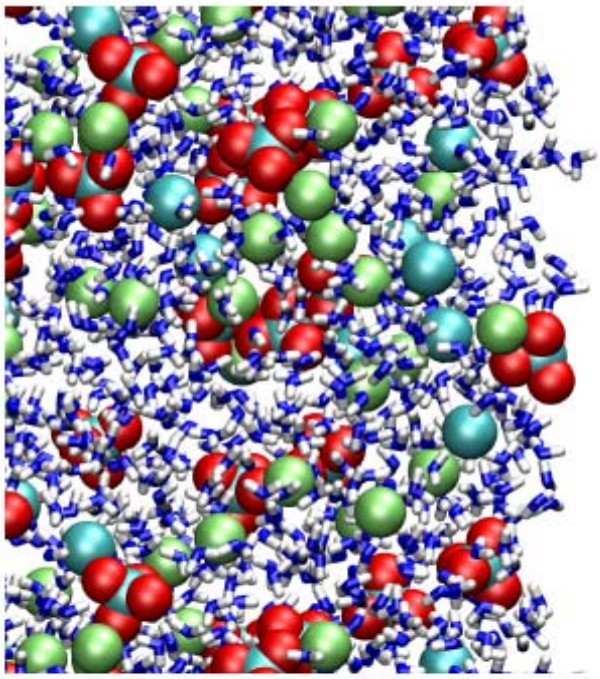

Figure 3

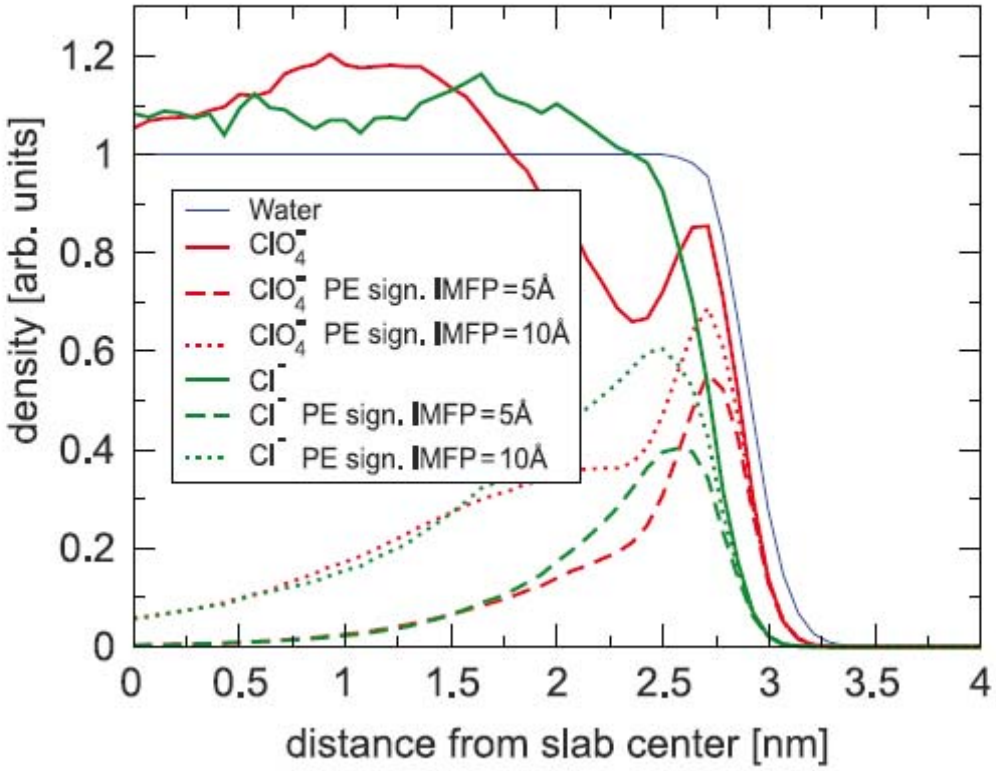
density [arb. units]
distance from slab center [nm]
Water
ClO4-
ClO4- PE sign. IMFP=5Å
ClO4- PE sign. IMFP=10Å
Cl-
Cl- PE sign. IMFP=5Å
Cl- PE sign. IMFP=10Å
0
0.2
0.4
0.6
0.8
1
1.2
0
0.5
1
1.5
2
2.5
3
3.5
4

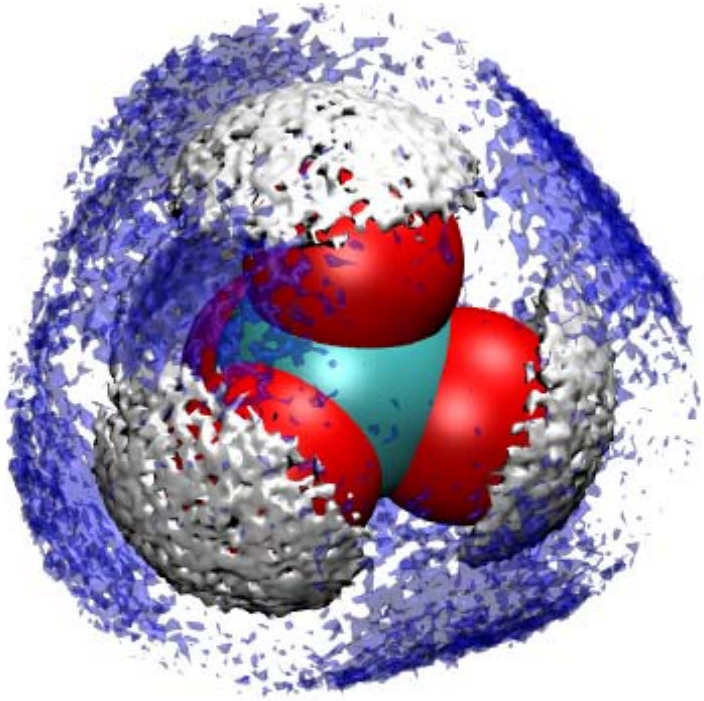

Figure 5